Continental Shelf Research 42 (2012) 51–63

Contents lists available at SciVerse ScienceDirect

Continental Shelf Research

journal homepage: www.elsevier.com/locate/csr

Research papers

Storm-induced inner-continental shelf circulation and sediment transport: Long Bay, South Carolina

John C. Warner [a,*], Brandy Armstrong [a], Charlene S. Sylvester [a,1], George Voulgaris [b], Tim Nelson [b], William C. Schwab [a], Jane F. Denny [a]

[a] Coastal and Marine Geology Program, US Geological Survey, 384 Woods Hole Road, Woods Hole, MA 02543, USA
[b] Department of Earth and Ocean Sciences, Marine Science Program, University of South Carolina, Columbia, SC 29208, USA

ARTICLE INFO

Article history:
Received 12 January 2011
Received in revised form
23 April 2012
Accepted 1 May 2012
Available online 11 May 2012

Keywords:
Sediment transport
Long Bay
South Carolina
Storm fronts

ABSTRACT

Long Bay is a sediment-starved, arcuate embayment located along the US East Coast connecting both South and North Carolina. In this region the rates and pathways of sediment transport are important because they determine the availability of sediments for beach nourishment, seafloor habitat, and navigation. The impact of storms on sediment transport magnitude and direction were investigated during the period October 2003–April 2004 using bottom mounted flow meters, acoustic backscatter sensors and rotary sonars deployed at eight sites offshore of Myrtle Beach, SC, to measure currents, water levels, surface waves, salinity, temperature, suspended sediment concentrations, and bedform morphology. Measurements identify that sediment mobility is caused by waves and wind driven currents from three predominant types of storm patterns that pass through this region: (1) cold fronts, (2) warm fronts and (3) low-pressure storms. The passage of a cold front is accompanied by a rapid change in wind direction from primarily northeastward to southwestward. The passage of a warm front is accompanied by an opposite change in wind direction from mainly southwestward to northeastward. Low-pressure systems passing offshore are accompanied by a change in wind direction from southwestward to southeastward as the offshore storm moves from south to north.

During the passage of cold fronts more sediment is transported when winds are northeastward and directed onshore than when the winds are directed offshore, creating a net sediment flux to the north–east. Likewise, even though the warm front has an opposite wind pattern, net sediment flux is typically to the north–east due to the larger fetch when the winds are northeastward and directed onshore. During the passage of low-pressure systems strong winds, waves, and currents to the south are sustained creating a net sediment flux southwestward. During the 3-month deployment a total of 8 cold fronts, 10 warm fronts, and 10 low-pressure systems drove a net sediment flux southwestward. Analysis of a 12-year data record from a local buoy shows an average of 41 cold fronts, 32 warm fronts, and 26 low-pressure systems per year. The culmination of these events would yield a cumulative net inner-continental shelf transport to the south–west, a trend that is further verified by sediment textural analysis and bedform morphology on the inner-continental shelf.

Published by Elsevier Ltd.

1. Introduction

Long Bay is a sediment-starved embayment located along the eastern coasts of North and South Carolina, USA (Fig. 1). Parts of this region are heavily developed with a strong history for tourism, fishing, and coastal activities. The rates and pathways of sediment transport are important to coastal communities because they are a fundamental component of the coastal sediment budget which, in turn, controls beach erosion and accretion patterns, determine the availability of sediments for planned beach nourishment projects, define seafloor habitat, and can negatively impact commercial and recreational marine navigation. Beach nourishment is often the primary tool for mitigating coastal erosion in the region and its success and cost depends on the availability of quality sand resources found on the adjacent continental shelf and minimizing the impact of utilizing these sand deposits. Understanding the processes that control the movement of sediment of the entire Long Bay system will provide coastal planners with better information to manage the system.

Long Bay extends from Cape Romain in the south, past the NC/SC border, and extends northward to Cape Fear. This bay features several inlets in the southern portion (such as Winyah

* Corresponding author.
E-mail address: jcwarner@usgs.gov (J.C. Warner).
[1] Current address: USACE Mobile District/Joint Airborne Lidar Bathymetry Technical Center of Expertise, 7225 Stennis Airport Road, STE 100, Kiln, MS 39556, USA.

0278-4343/$ - see front matter Published by Elsevier Ltd.
http://dx.doi.org/10.1016/j.csr.2012.05.001

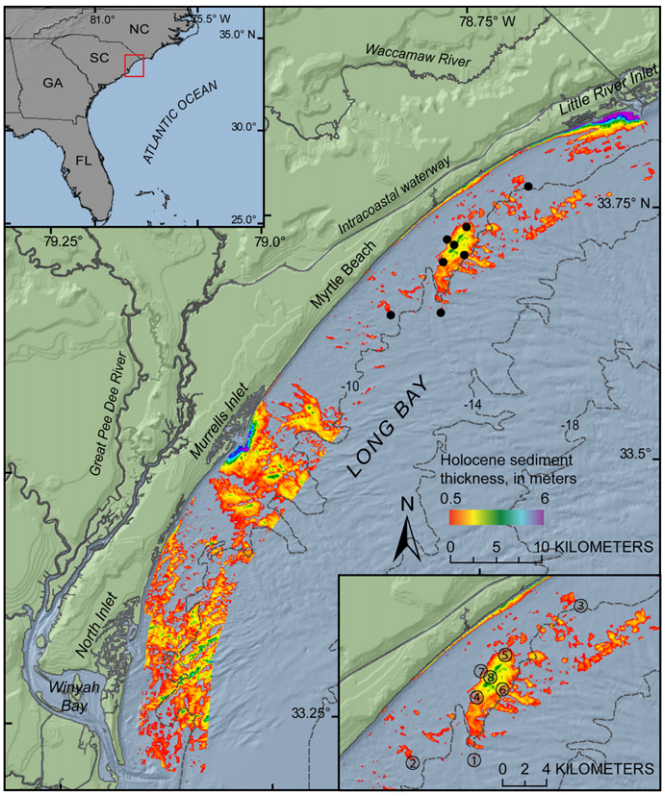

Fig. 1. Coastline of South Carolina showing bathymetric contours and locations of equipment deployed at the study site. Colors identify resolvable surficial sediment thickness (> 0.5 m) from Denny et al. (2005). Lower right inset identifies detailed locations of equipment deployments. (For interpretation of the references to color in this figure legend, the reader is referred to the web version of this article.)

Bay, North Inlet, Murrells Inlet, and Little River Inlet; Fig. 1). This region is part of a cuspate shaped coastline that includes Long, Onslow, and Raleigh Bays delineated by Cape Romain, Cape Fear, Cape Lookout, and Cape Hatteras. The majority of the Carolina Capes region is bounded to the west by low-lying barrier islands. Although there is limited significant freshwater discharge in Long Bay, Cape Fear to the north and the Pee Dee River to the south provide periodic intrusions of freshwater. The continental shelf along the southeastern coast of the USA, usually referred to as the South Atlantic Bight (SAB), has been identified as a region with three distinct hydrodynamic regimes (Atkinson et al., 1983; Lee et al., 1985). These are: (1) the inner-continental shelf, where local winds and river runoff are the primary forces; (2) the mid-shelf (20–40 m water depth), where local winds dominate the flow at sub-tidal frequencies and with a seasonally varying stratification; and finally (3) the outer-continental shelf, where Gulf Stream meanders influence the observed flows. This characterization was based on observations obtained mainly along the shelves of Georgia and North Carolina (Atkinson et al., 1983; Atkinson and Menzel, 1985; Werner et al., 1993). Measurements in the inner-continental shelf of Onslow Bay showed that semidiurnal tidal processes are responsible for approximately 50% of the kinetic energy of the currents, while about 45% was attributed to long-period atmospheric and random oceanic processes. In the mid-shelf portion of the SAB, it has been shown (Tebeau and Lee, 1979; Lee and Brooks, 1979) that tidal currents account for 80–90% of the total cross-shelf and about 20–40% of the along-shelf variation. In the inner-continental shelf, which is of interest here, energy at semidiurnal frequencies dominates the cross-shore variance (Pietrafesa et al., 1985).

A band of low salinity water, termed a frontal zone, occupies the inner-continental shelf from the shoreface to a distance 10–20 km offshore. Observations indicate that the freshwater frontal zone can persist for most of the year and that the resulting density gradient can form a dynamic barrier inhibiting the transport of low salinity water from the inner-continental shelf farther offshore (Blanton, 1981). The frontal zone is responsive to wind forcing (Atkinson et al., 1983; Blanton and Atkinson, 1983). Southward winds cause the low salinity zone to form a dynamic barrier that separates inner-continental shelf circulation from current motions over deeper portions of the shelf. With northward winds, surface waters are transported across the continental shelf ejecting low salinity water and replacing it with more saline water from below (for example, upwelling). Schwing et al. (1983) suggested that this does not apply to the region north of Cape Romain, however freshwater plumes have been noted in Onslow Bay (north of Long Bay) and the Cape Fear River can introduce significant quantities of freshwater into the coastal ocean, north of the study area. Gutierrez et al. (2006) identified a two-layered flow regime attributed to the presence of stratification and was favored during upwelling winds (towards the north–east). During down-welling conditions vertical mixing removes the two-layered regime.

Previous studies have characterized the shallow geologic framework on the inner-continental shelf and nearshore regions of Long Bay (Baldwin et al., 2004, 2006; Denny et al., 2005; Barnhardt, et al., 2007; Schwab et al., 2008; Denny et al., in press). The coast consists of generally thin and narrow sandy Holocene beaches that overly Pleistocene and older fluvial channel fill and Cretaceous- and Tertiary-age coastal plain sedimentary strata. Offshore the sandy Holocene sediments form a patchy and discontinuous veneer that is sufficiently thin across much of the inner-continental shelf to allow exposure of these older underlying sedimentary units on the seafloor. These studies identified several large sand shoals on the inner-continental shelf seaward of active tidal inlet system, such as North Inlet, Murrells Inlet, and Little River Inlet (Fig. 1). The shoals are interpreted as the landward retreat paths of the inlet systems over the course of Holocene sea-level rise. One relatively large sand shoal offshore of Myrtle Beach is not associated with a currently-active inlet system. This shoreface-detached shoal feature is oriented oblique to the coastline and is approximately 10 km long, 2 km wide, and in excess of 3 m thick. This feature is also thought to have formed as the retreat sand sheet of an inlet system that gradually lost tidal prism as it transgressed and was eventually overridden by the active beach system (Barnhardt et al., 2007; Denny et al., in press). It is unclear how modern inner-continental shelf processes have modified or are maintaining the shoal.

The processes that are responsible for controlling sediment transport on the inner-continental shelf are typically wind and wave dominated. Previous investigations have identified the ocean circulation on the inner-continental shelf of Long Bay as strongly influenced by river runoff and atmospheric forcing and highly responsive to wind forcing (Atkinson et al., 1983). Austin and Lentz (1999) found that the passage of cold fronts, warm fronts, and low-pressure systems have a distinctive influence on inner-continental shelf weather systems and contribute to meteorological variability on the timescale of days to weeks. The duration, magnitude, and frequency of the atmospheric forcing caused by these storm types will dictate the long-term sediment fluxes of the region.

In this paper we utilize observational data to describe processes that lead to the mobilization and transport of sediment on the inner-continental shelf of Long Bay, SC. The paper is outlined with Section 2 describing the observational program, Section 3 characterizes the different storm types based on data analysis, Section 4 describes the frequency recurrence interval for the storm types, and Section 5 is the conclusions.

Table 1
List of sensors from site 7 (~10.5 m) specific to this analysis (taken from Sullivan et al., 2006). (*cmab=cm above bottom).

Sensor	Instr height (cmab*)	Sampling rate (hz)	Sampling interval	Accuracy
(1) Rotating sonar	53	–	5 hr	± 0.01 m
(2) ADVs	53, 54	8	3600 s	<0.3 cm s^{-1}
(3 beam) ABS's	103	64	3600 s	–
(1) PCADP	102	1	3600 s	<1.0 cm s^{-1}
(1) ADCP	206	1	900 s	<1.0 cm s^{-1}
(2) Pressure	169, 172	1	3600 s	2.0 cm
(1) CT	174	–	3600 s	0.0003 S m^{-1}, <0.2 C

2. Observations

Oceanographic equipment was deployed at eight sites from October 2003 to April 2004 on the inner-continental shelf offshore of Myrtle Beach, SC. The instruments were focused on the offshore sand body that is associated with the 10 m isobath (Fig. 1 and inset). Sites 6-8-7 and 4-8-5 were established to provide transects across and along the shoal. Site 1 was at an offshore location to acquire approaching wave fields and sites 2 and 3 were the far field sites located along or near the 10 m isobath.

Instruments were deployed on tripods at each site to measure average surface wind–wave properties, water level, currents, temperature, and salinity. Two of the tripods (sites 6 and 7) additionally were equipped with instrumentation to measure bed forms (ripples) using a rotary sonar, acoustic Doppler velocimeters (ADV) to measure near-bottom turbulence, acoustic backscatterance sensors (ABS) to measure suspended-sediment concentrations, and site 7 was also equipped with a pulse coherent acoustic Doppler profiler (PCADP). The ABS's were calibrated in a 2 m tall and 50 cm in diameter recirculating tank equipped with a pneumatic diaphragm pump, located at the University of South Carolina. Because the ABS was a multi-frequency system we utilize the response of the different frequencies to obtain information on both particle size and concentration. In order to do that the ABS system constants were estimated using a calibration technique for scatterers with well known size and acoustic properties. Glass spheres are used for this purpose as described in Thorne and Hanes (2002), and Thorne and Campbell (1992).

Details of the deployment, site locations, equipment specifications, all the processed data, and the processing tools are described in Sullivan et al. (2006) and provided at http://pubs.usgs.gov/of/2005/1429/. The 6-month deployment included a mid-term cleaning/turnaround in mid January. At that time it was identified that a majority of the equipment had encountered severe biological fouling which greatly reduced the usefulness of the data for the first half of the deployment. This manuscript will focus mainly on the second half of the data set (from mid Jan to April 2004), with an emphasis on data collected at site 7, with equipment as listed in Table 1.

3. Results

3.1. Meteorological and oceanographic setting

Prevailing wind directions in the region are nearly shore-parallel and represent the directions of the strongest, on average, winds. Northeastward winds, upwelling favorable, occur mainly in the summer while during October the winds are towards the south–west and are downwelling favorable. In general, the alongshore structure of the currents and the coastal sea surface variations in the SAB have been found to respond to local winds (Werner et al., 1993). During the deployment strong winds occur towards both the north–east and south–west (Fig. 2A). The wind speeds (Fig. 2B; wind towards) reached 10–15 m s^{-1} during the peak of the storms and there is a high correlation with wave height (Fig. 2B). It is characteristic that wave conditions are in response to local wind forcing and not swells or other waves generated outside the region. This is in part due to the wide inner-continental shelf of Long Bay which can dissipate most background longer period swell that may propagate landwards from the mid-Atlantic (this is excluding hurricanes). Wave heights during the study period rarely reached 2 m at this location (10 m water depth), and sustained a background level of 20–30 cm.

The tides in this region are semidiurnal with a range of approximately 1.4 m (Fig. 2C). The low frequency low-pass (30 h) filtered water level (red line, Fig. 2C) shows variability correlated with the local wind field. During periods of local sustained winds towards the south–west the free surface experiences a measurable increase in water level (for example February 29) and periods of winds towards the north–east (for example March 5) which produced a relative set-down in water level, though to a lesser extent.

Currents on the Long Bay inner-continental shelf are predominately wind forced flows with a weaker tidal influence. Data collected by Gutierrez et al. (2006) during a previous deployment in Long Bay demonstrates that the relative contribution of the alongshore and cross-shore components of tidal flow depends on the distance from the shore. In general, the cross-shore component of the tidal current contributes only 15% to the total current variability near the coastline (within 1 km) and increases further offshore (82% at 10 km from the shoreline). The relative tidal contribution of the along-shore current varies from 35% near the shore (within 1 km) to only 18% 10 km away from the coastline. The current data was projected to a shore parallel (positive heading towards 47° true) and cross-shore (positive heading onshore towards 307° true). During our deployment the alongshore surface currents rarely exceeded 20 cm s^{-1} and were strongly influenced by the local winds (Fig. 2D). For example, sustained winds towards the south–west during the storm near February 29 drove a current to the south–west reaching 20 cm s^{-1} with tidal fluctuations on the order of 5 cm s^{-1}. Similarly, winds toward the north–east, for example near March 5, drove a weaker flow along the wind direction. In the cross-shore direction the observed currents are ± 10 cm s^{-1} and appear to be primarily driven by tides and weakly influenced by the alongshore-directed wind stress (Fig. 2E).

3.2. Sediment characteristics

Surficial sediment samples were obtained at each site using a Van Veen-type grab sampler. The samples were sieved to determine a grain size distribution following the methodology outlined in Poppe et al. (1985). Results show a relatively consistent distribution between the sites with grain sizes ranging from ~0.125 mm (3ϕ) to ~1.0 mm (0ϕ), with a mean size of $d_{50}=0.35$ mm. An exception is at site 7, which was skewed towards a finer grain size distribution with a mean size of 0.18 mm.

Sediment is mobilized primarily due to bottom stress from locally generated waves. The mobility stress, expressed as a shear velocity u^*, was computed using Madsen (1994) using locally measured waves from the ADCP and near bed currents from the ADV at site 7 and a grain size based on d_{50}. The shear velocity

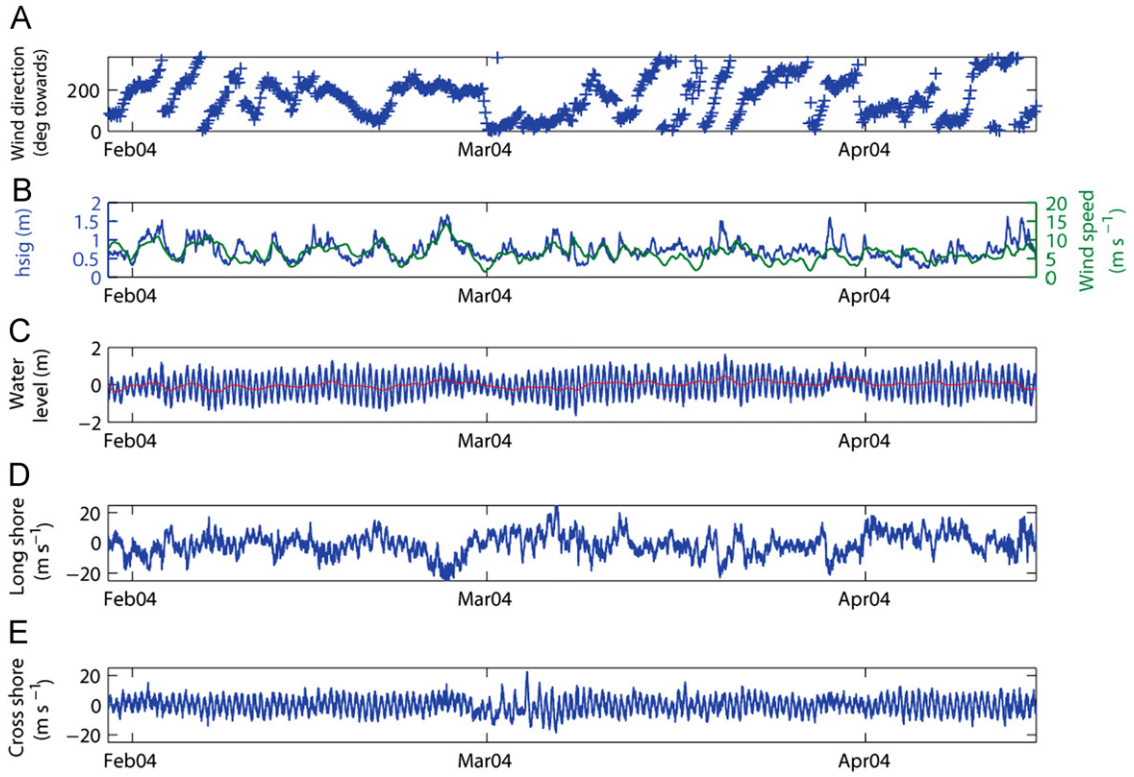

Fig. 2. Time series of (A) wind direction (towards); (B) wind speed and wave heights; (C) instantaneous and filtered water levels; (D) along-shore current speed; and (E) cross-shore currents. (For interpretation of the references to color in this figure legend, the reader is referred to the web version of this article.)

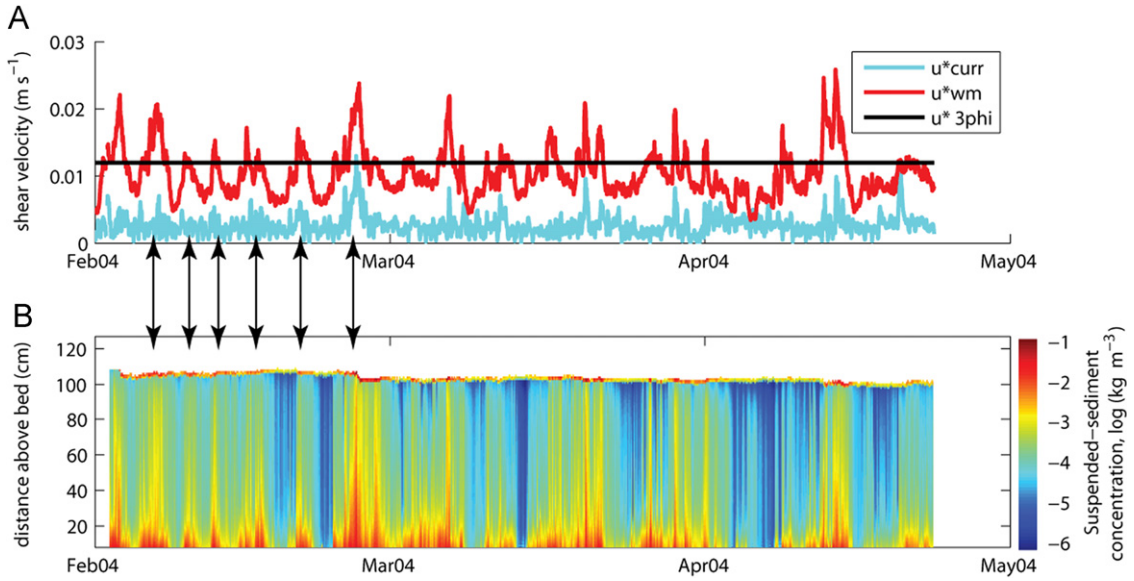

Fig. 3. Time series of observed (A) current shear velocity (u*curr), combined wave-current shear velocity (u*wm), and mobility shear velocity for 3ϕ; and (B) vertical profiles of suspended-sediment concentration log scale. Vertical arrows relate some of the wave-current bottom stress events to the increased sediment concentration profiles. (For interpretation of the references to color in this figure legend, the reader is referred to the web version of this article.)

from the currents alone (u*curr) and the shear velocity for the combined maximum wave and currents (u*wm) are shown in Fig. 3A. Based on Soulsby and Whitehouse (1997), the shear velocity required to mobilize the finest grain size (3ϕ) is 0.012 m s^{-1} (horizontal black line in Fig. 3A). It can be seen that the shear velocity for the currents alone (cyan line in Fig. 3A) rarely increases to the threshold to mobilize the sediment. This identifies that the currents alone are not strong enough to mobilize sediment on the inner-continental shelf at this location. However, with the presence of waves, the maximum combined velocity (red line in Fig. 3A) regularly exceeds the threshold for mobility for the 3ϕ. The combined shear velocity is highly correlated with the waves and therefore identifies that the waves are the dominant factor for mobility of sediment on the inner-continental shelf. Once mobilized, the sediment will be transported by the mean currents due to both the tides and wind driven flows.

Time series profiles of suspended-sediment (Fig. 3B) demonstrate the resuspension of bottom sediments. Increased water column concentrations are correlated with the combined wave-current shear velocity (vertical arrows Fig. 3B). Profiles show a vertical distribution with maximum values near the seafloor and decreasing through the water column. During periods when the stress is less than the critical value, there is limited resuspension and concentrations are small. After the sediment is resuspended into the water column, the wind and tidal driven currents will transport the material. As shown previously, these currents are a function of the wind direction, which is a function of the type of storm that is impacting the region. To understand the net sediment transport directions an understanding of the different storm patterns is required.

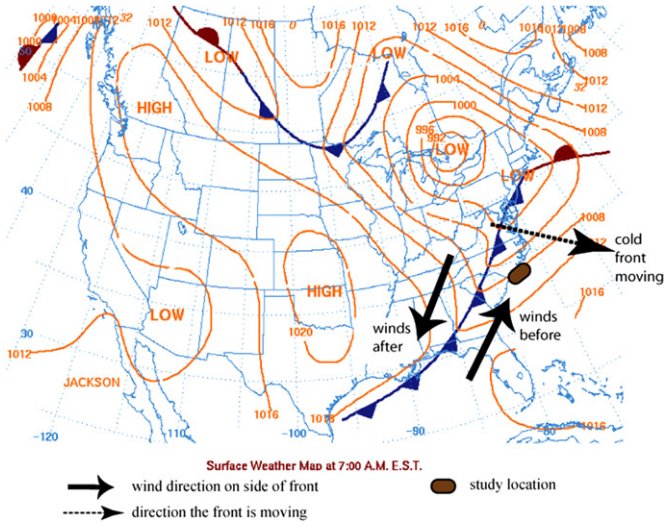

Fig. 4. Example of a Cold Front http://www.hpc.ncep.noaa.gov/dailywxmap. (For interpretation of the references to color in this figure legend, the reader is referred to the web version of this article.)

3.3. Storm pattern observations

The free surface, currents, and suspended sediment all are modulated significantly by the local wave and wind fields. Following a general description by Austin and Lentz (1999), the wind fields in this region can be associated with three types of storm patterns driven by cold fronts, warm fronts, or a low-pressure system directly. In the northern hemisphere, a region of low pressure is comprised of counter-clockwise rotating winds. These winds transport cooler air from the north to the south and create a trailing cold front that extends southward from the low pressure. The winds also drive warm air from the southeast to the north and create a warm front that extends eastward from the low pressure. The passage of theses fronts over the study region create distinct weather patterns. Additionally, the low-pressure system directly, or a low-pressure that develops offshore, can impact the study region. The meteorological conditions and

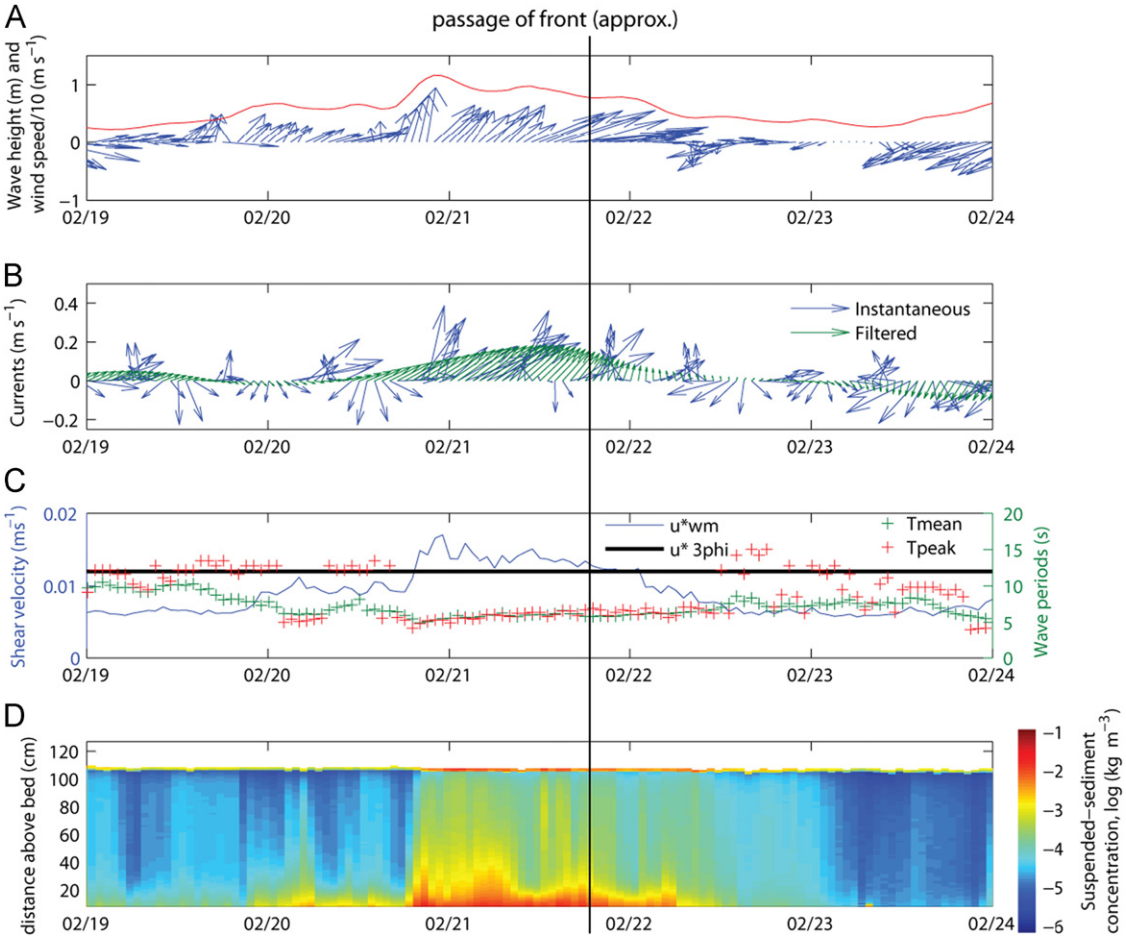

Fig. 5. Detailed measured response during the passage of a cold front. Time series of (A) wave heights and winds (arrows); (B) instantaneous and filtered currents; (C) combined wave-current bottom shear velocity and 3ϕ threshold, wave periods; and (D) profiles of suspended-sediment concentration. (For interpretation of the references to color in this figure legend, the reader is referred to the web version of this article.)

details of the observed inner-continental shelf response for each storm pattern are presented in this section.

3.3.1. Cold front

One type of storm system that impacts the region is a cold front. Cold fronts are characterized as regions of strong temperature gradients with large variations in wind speed and direction. This storm type occurs when a low-pressure system travels from west to east, north of the study area, and the trailing cold front passes over the study area. Fig. 4 shows such a cold front on February 21, 2004 exhibiting a typical pattern with a low pressure in the northern US and trailing cold front to the south shown with a blue line and triangles pointing in the direction of travel (images from http://www.hpc.ncep.noaa.gov/dailywxmap). The study region is identified with a brown ellipse in Fig. 4. The circulation around the low is counterclockwise so the study area will first encounter winds blowing towards the north–east "winds before" arrow. After passage of the front the air temperature drops and the winds shift toward the southeast "winds after" arrow.

The passage of the cold front creates a distinctive response as observed during a 5-day period from February 19 to 24 (Fig. 5). The winds first are towards the north–east (arrows, Fig. 5A) and the wave heights peak early (red line) because the winds are blowing over a longer fetch than when they shift and blow offshore. Following the front passage the winds shift towards the southeast and because the wind is now blowing from the land the wave heights decrease. The instantaneous currents (blue arrows, Fig. 5B) demonstrate tidal oscillations but the subtidal mean current is towards the north–east (green arrows). Both the mean and peak wave periods decrease to about 6 s (Fig. 5C) during the storm. The combined wave-current bottom shear velocity peaks at near 0.015 m s^{-1} when the wave heights are the strongest near the beginning of the storm. When that bottom shear velocity exceeds the threshold of 0.012 m s^{-1} (threshold for mobilization of particles with diameter of 3ϕ) the sediment is resuspended (Fig. 5D). The bottom shear velocity value is maintained above the threshold level for motion until the winds shift towards the southeast on February 22. As the winds rotate due to the passage of the front, the wave heights decrease and the bottom shear velocity reduces below the threshold value for resuspension. The vertical suspended-sediment profiles are strongly correlated with the bottom shear velocity time series. The largest concentrations occur during the leading part of the storm when the waves are greatest. The concentrations remain elevated until the 6th hour of Feb 22, a few hours after the shear velocity falls below the threshold value, allowing the sediment to settle out of the water column. The net sediment flux during this cold front was found to be towards the north–east because the mean current was in that direction and the sediment concentrations were higher during the leading part of the storm.

Rotary sonar data was analyzed to determine the wavelength and orientation of the bedform ripples as they evolved through time (Fig. 6). The wavelengths and orientations were first determined by hand calculations on printed images, and then compared to a subsequent automated method based on Voulgaris and Morin (2008). The method separates each image into eight boxes radially distributed around the circle, overlapping and scaled to maximize the amount of enclosed area. It then uses a 2D Fast Fourier Transform (FFT) routine to analyze the set of boxes, choosing the dominant frequency and interpreting that wave geometrically to calculate the wavelength and orientation. The ripple wavelengths varied from 0.2 m in between storms and decreased to less than 0.1 m during the storm events (Fig. 6A). Ripple directions are seen to rotate during each storm (Fig. 6B). The colors identify the storm types and are described in Section 3.4. During cold fronts (blue shaded areas) the ripple direction typically rotates to be pointing in a more northerly direction

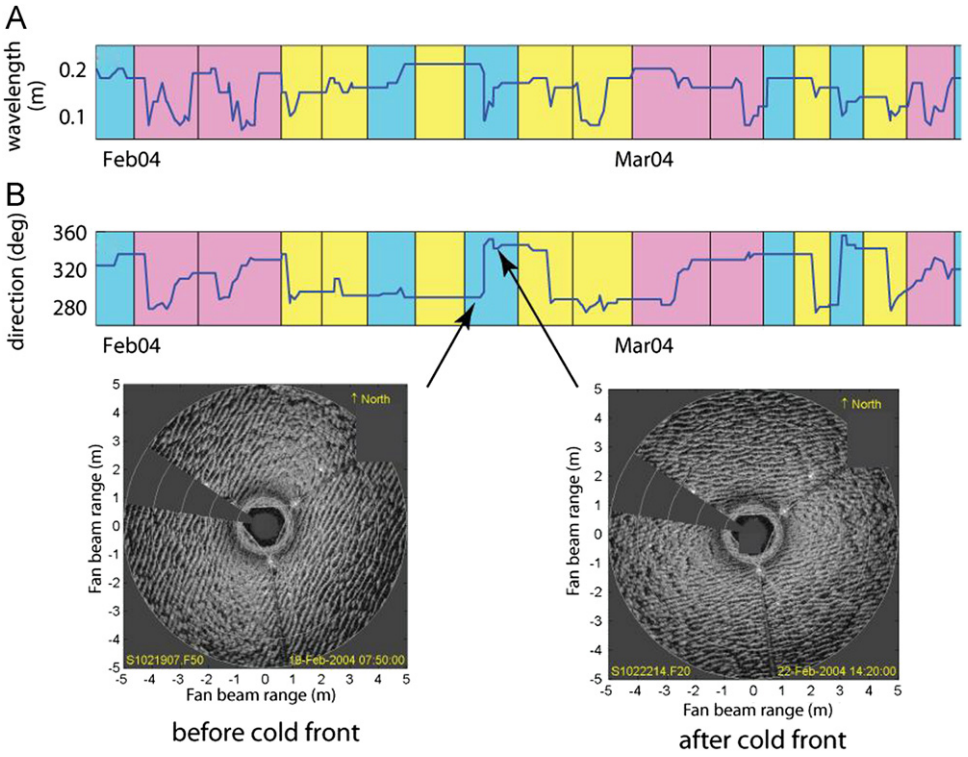

Fig. 6. Time series of (A) ripple wavelength and (B) direction (crest perpendicular). Shading represents storm type (blue=cold front, red=warm front, yellow=low-pressure system, described in Section 3.4). Bottom row: seafloor sonar images showing ripple orientations before and after passage of cold front. (For interpretation of the references to color in this figure legend, the reader is referred to the web version of this article.)

(~350 deg) by the end of each cold front storm. These directions are defined as being perpendicular to the ripple crests, with an example as shown in Fig. 6 bottom panels.

The bottom two panels (Fig. 6) are seafloor images from the rotary sonar. Each image shows the backscatter in a 5 m radius from under the tripod. There is a shadow zone to the left on each image because the sonar does not rotate a full circle. The shadow is near one of the tripod legs and the other two legs are visible. The images identify ripple patterns on the seafloor. Before the storm the ripples are orientated in a NE–SW alignment (left panel) with a direction of 290°. During the peak of the storm the ripples become more disorganized as the sediment moves in suspended and sheet flow regimes (not shown), however there is already a trend for the ripples to re-align themselves towards an E–W direction due to the predominant wave direction being towards the north–east. As the storm subsides (right panel) the ripples reorganize themselves into an almost E–W orientation, with a direction of 350°, consistent with the strongest wave direction during the storm. The waves generated by the back side of the front were not strong enough to re-orientate the ripples patterns.

3.3.2. Warm front

Another type of storm system is the passage of a warm front, also characterized by a region of low-pressure similar to that described previously for the cold front case. However this time the low-pressure system is to the west of the study area and travels to the north (Fig. 7). The warm front extending eastward from the low-pressure center will travel over the study area from south to north. The front passage provides an increase in wind magnitude that rotates, typically with winds first heading towards the south–west (or south–east) and then rotating towards the north–east. These wind directions also switch as in the passage of the cold front, but in the opposite direction. The atmospheric pressure will decrease to a minimum with the front passage and this minimum in pressure coincides with a maximum in air temperature (not shown).

The details of the inner-continental shelf response for the warm front (Fig. 8) have some similarities as shown previously. Winds are first towards the south–west and after the front passes they rotate towards the north–east (Fig. 8A). Wave heights reach to over 1 m and are sustained for the duration of the event, with almost equal magnitude on both sides of the front. The currents still exhibit a strong tidal signal, however there is a stronger net flow to the north–east after the passage of the front, most likely due to stronger winds at that time (Fig. 8B). The bottom shear velocity

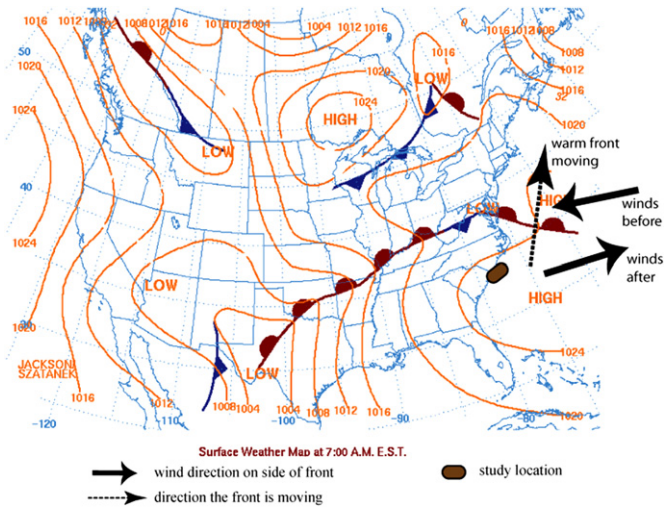

Fig. 7. Example of a Warm Front http://www.hpc.ncep.noaa.gov/dailywxmap.

reaches the 3φ critical threshold for resuspension near the start of the storm event on February 5 (Fig. 8C) and remains near that threshold level for the leading part with winds toward the south–west. Near and after passage of the front the winds shift and the bottom shear velocity increases to nearly 0.02 m s^{-1}. This stress increase is caused by an increase of the apparent roughness due to waves as the near bed wave period increase from ~6 s to ~8 s after the passage of the front. This is caused by the longer fetch than when the winds are blowing offshore allowing the generation of longer period waves (Fig. 8C). The suspended-sediment (Fig. 8D) has relatively large concentrations on both sides of the front, but greater concentrations occur after the front passes because the bottom stress is greater after the front. The net sediment flux for the warm front was almost equal in both directions with a slightly larger flux towards the north–east because the sediment concentrations were larger on the back side of the storm when the currents were heading in that direction. The seafloor ripple directions from the sonar sensor (Fig. 6B) show that the ripple directions are typically re-orientated towards ~340° after all the warm fronts (pink shading). This is a consistent pattern except for perhaps the first warm front event that reorients them from 340 to 320, but still heading in a northerly direction at the end of the storm.

3.3.3. Low-pressure systems

A low-pressure system is characterized by a region of lower pressure that typically develops offshore of the study area and travels from south to north, to the east of Long Bay (Fig. 9). These low-pressure systems may or may not have associated fronts, and can take the form of tropical systems or Nor'Easters. Winds shift from southwestward to southeastward as the low passes, and maintain a southerly direction across the study region. The atmospheric pressure and air temperature do not show a similar response as for the cold and warm fronts because a temperature front is not necessarily passing over the study region. We also include Nor'easters in this category, as they are characterized by continuously strong winds blowing towards the south–west, and the coastal system exhibits a similar response as to tropical systems.

The details of the inner-continental shelf response for the low-pressure systems (Fig. 10) are different than for the fronts. The winds do not shift in the N–S direction but maintain a constant south–west or south–east direction (Fig. 10A). Wave height increases with the wind stress and reaches a maximum during the latter part of the storm (Fig. 10A) and then decrease as the storm subsides. The currents respond with the development of constant southerly subtidal flow superimposed on the tidal oscillation (Fig. 10B). Combined wave-current bottom shear velocity peaks with the wave height and exceeds the critical threshold for 3ϕ mobility during most of the event. Near the end of the storm the wave heights decrease but the wave period increases and this sustains the bottom stress above critical level (Fig. 10C). Vertical profiles of suspended-sediment are correlated with the bottom shear velocity (Fig. 10D) showing a sudden increase on February 25 at noon and momentary decrease later on the 25th when the stress temporarily decreases below incipient motion. The net sediment flux for low-pressure systems is towards the south–west because that is the primary direction during the whole event. The seafloor ripples (Fig. 6) started out in almost an E–W orientation for this event, remnant from the previous storm event. During the storm the ripples were washed out due to the intense sediment transport but they quickly re-established themselves. At the end of all the low-pressure systems, the ripples were orientated to be heading towards 270–290°. Relative to the coastline, this would be towards the south–west. This direction correlates with a refracted onshore wave direction during the low-pressure system.

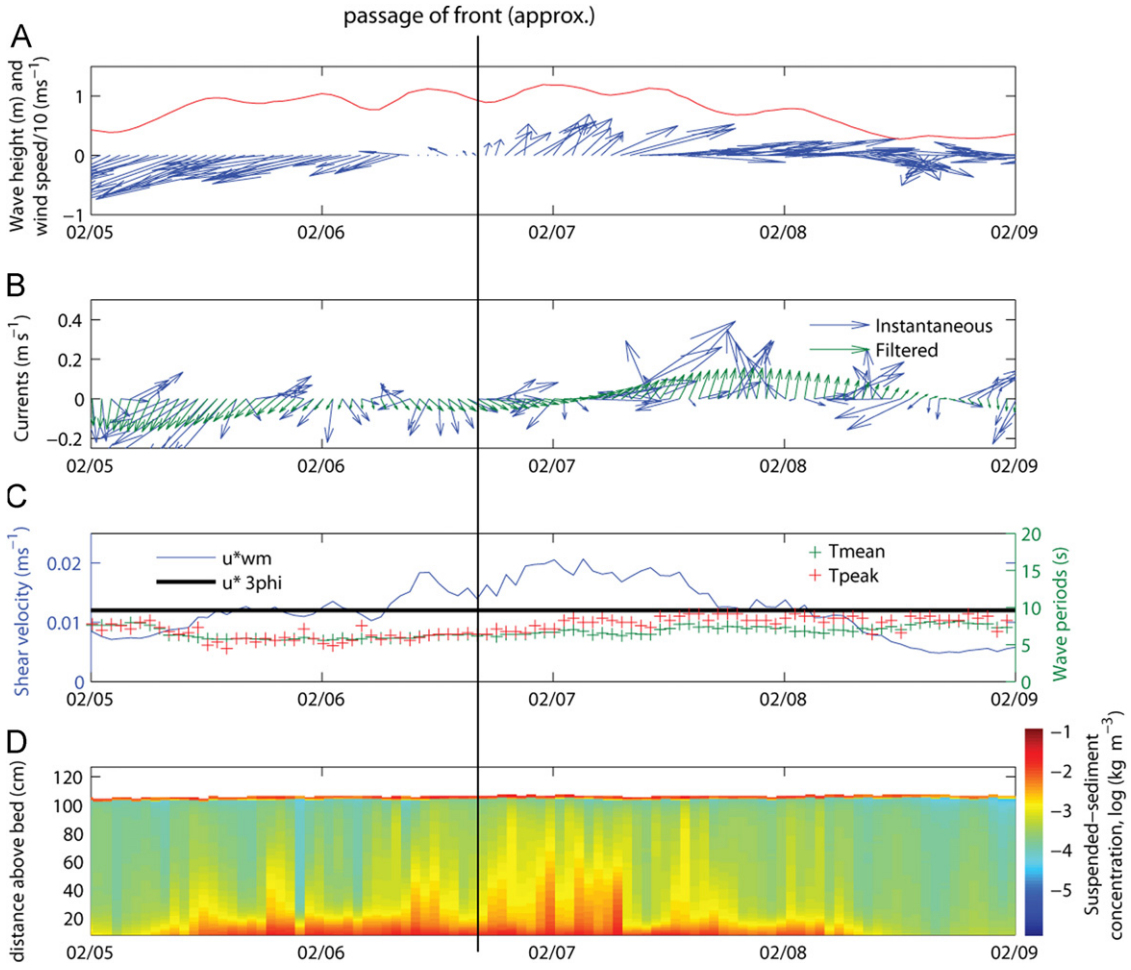

Fig. 8. Detailed measured response during the passage of a warm front. Time series of (A) wave heights and winds (arrows); (B) instantaneous and filtered currents; (C) combined wave-current bottom shear velocity and 3ϕ threshold, wave periods; and (D) profiles of suspended-sediment concentration.

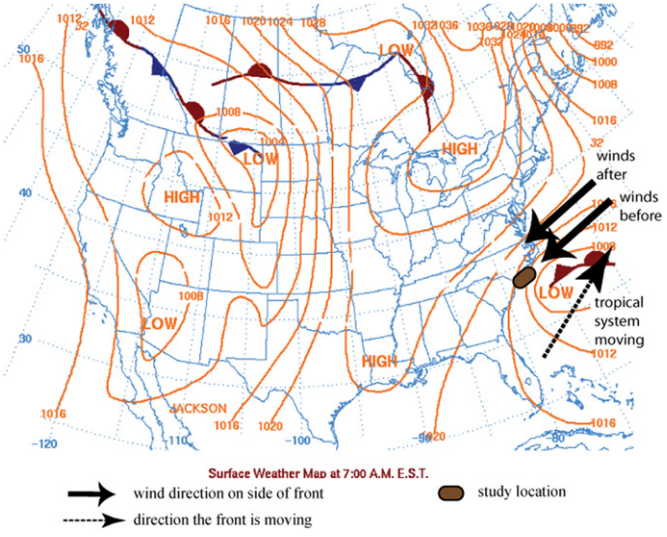

Fig. 9. Example of a low-pressure system storm type, http://www.hpc.ncep.noaa.gov/dailywxmap.

3.4. Storm classification and analysis

Each storm type produced a different response from the currents, waves, and sediment transport on the inner-continental shelf. In order to understand the cumulative effect of these different types of events, we initially applied some strict criteria to categorize each storm type and subsequently determine the recurrence of each type using data from a variety of sources and an analysis method that is described in the next section.

3.4.1. Available data

To categorize a longer term (~10 year) record of storm types, historical data from the National Data Buoy Center (NDBC) was acquired (http://www.ndbc.noaa.gov/historical_data.shtml) including significant wave height, wind direction, wind speed, air temperature and sea level pressure. This preliminary analysis was performed using NDBC 3 m discus buoy 41004, located 41 nautical miles south–east of Charleston, SC at 32.50 N 79.09W, where the water depth is 33.5 m. Data were recorded at this buoy for the years 1978–1982 and 1994–2006. This study focuses on the 1994–2006 data as these are the most complete records. Model data, as described below, were used to fill gaps in the observational data record.

NCEP North American Regional Reanalysis (NARR) 3-hourly data were downloaded from the NOAA Earth System Research Laboratory Physical Sciences Division website available at http://www.cdc.noaa.gov/cgi-in/db_search/SearchMenus.pl. The NARR data includes wind speed and direction, sea level pressure, and air temperature at 10 m.

Wave Watch 3 (WW3) data were downloaded from the National Oceanic and Atmospheric Administrations WW3 historical data page available at http://polar.ncep.noaa.gov/waves/nww3_hist.html. Time series were extracted from these data at

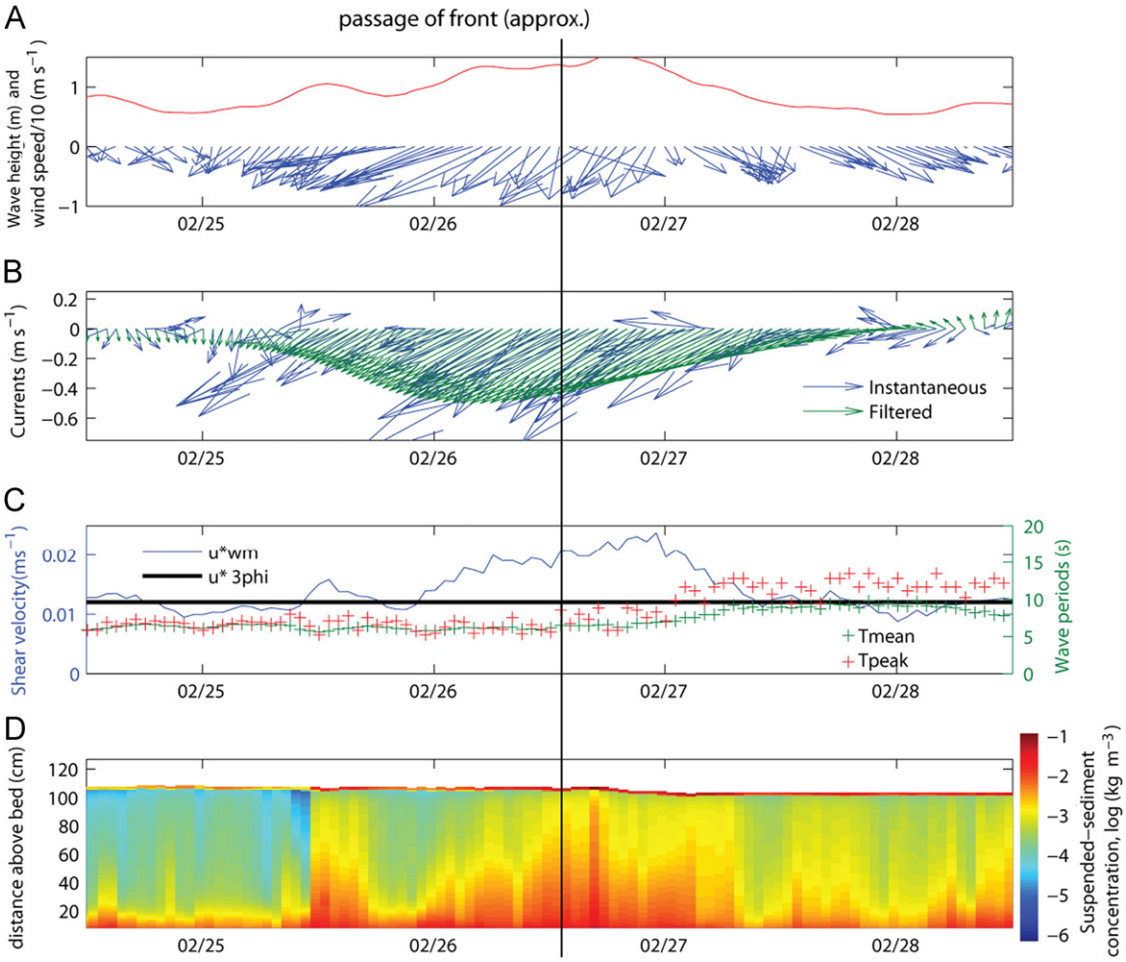

Fig. 10. Detailed measured response during the passage of a low-pressure system. Time series of (A) wave heights and winds (arrows); (B) instantaneous and filtered currents; (C) combined wave-current bottom shear velocity and 3ϕ threshold, wave periods; and (D) profiles of suspended-sediment concentration.

the closest point to the buoy. These data were available for 2001 through 2006 and were used to fill gaps in the NDBC significant wave height and peak wave period time series.

The NDBC data were cleaned to remove duplicates and all data was filtered using a low-pass filter with a period of 35 h to remove signals shorter than 2–3 day. The NARR and WW3 data were interpolated to the same sampling interval as the NDBC data (hourly) and used to fill any gaps in the buoy data record.

3.4.2. Storm definitions

Wave events or "storms" were preliminarily delineated as periods when the significant wave height rose above a baseline value of 0.5 m, and the start and end of each event was defined as the lowest wave height between events (Fig. 11). Some storms, particularly low-pressure systems, move or develop offshore and the fronts associated with these storms may not show up in the weather buoy data. Wave height was used as a preliminary criteria to help ensure that events were not omitted or misclassified in these situations. Lows in pressure were then used to define when a frontal boundary was present. Wave events with more than one pressure front were divided evenly between the two pressure fronts to become two events.

3.4.3. Classification methods

Analyses using periods of 24, 28 and 32 h were performed. Comparisons with composite surface maps from Unisys Weather, (12 h, 1996–2008 http://weather.unisys.com/archive/index.html) and NOAA Weather Maps (daily, 2002–2008 http://www.hpc.ncep.noaa.gov/dailywxmap/explaination.html) revealed that in cases where a cold front and a warm front followed in close succession, the shortest analysis period showed a bias towards warm fronts while the longest analysis period showed a bias towards cold fronts. The period that showed the least amount of bias, 28 h, was selected for the classification scheme.

3.4.4. Classification scheme

Following descriptions in Austin and Lentz (1999), a classification scheme was developed classify events that occurred over a time period of several years as cold fronts, warm fronts, or low-pressure systems. First the wave heights over the entire time period were used to delineate different storm event segments. Each segment was then processed through a procedure to determine the appropriate category (Fig. 11).

The first step was to determine if a low pressure was present in each segment. If there was no low pressure (follow "no low pressure" arrow, Fig. 11) the wind field was analyzed. If the wind direction before the front is towards the north and after the front is towards the south (N:S), it was classified as a cold front. If the wind direction before and after the front is primarily towards the north (N:N), it was classified as a warm front. This would identify that the front was predominately north of the study area. If wind direction before the low is towards the south and after is northward (S:N), or if wind before and after the front is primarily towards the south (S:S) it was classified as a low-pressure

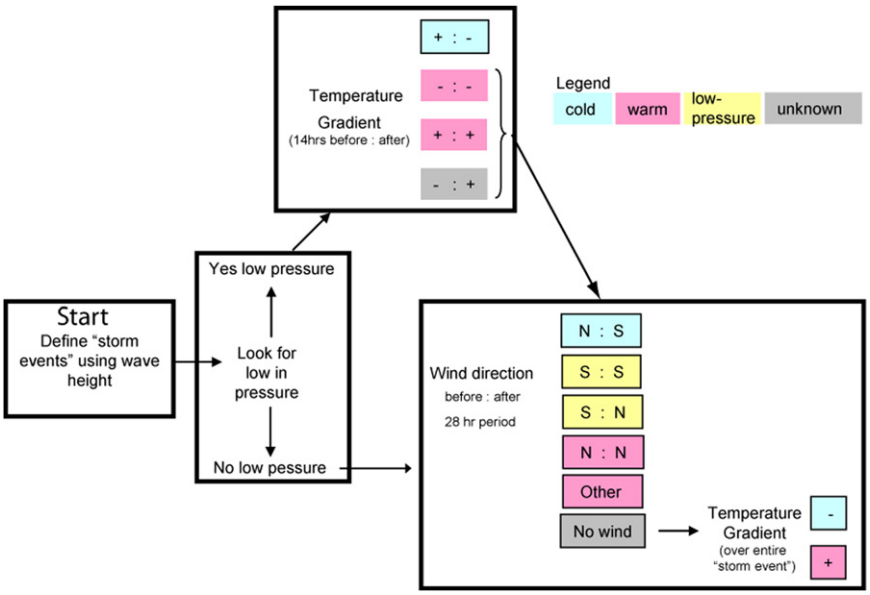

Fig. 11. Scheme to classify storms as cold front, warm front, or low-pressure system utilizing atmospheric pressure, temperature gradients, and average wind direction over a 28 h period (14 h before and after lows in pressure). Boxes with black outline represent final classifications.

systems. If wind data were available but could not be classified as cold or low-pressure system by direction, the front is classified as warm front. If wind data were not available, the front is classified depending on the temperature gradient. A decrease in temperature categorizes the event as a cold front and increase is classified as a warm front.

If a low pressure was detected (follow "yes low pressure" arrow, Fig. 11) then the time period 14 h before and after each low was analyzed to determine the dominant temperature and wind patterns.. If the temperatures were constant or decreased before and increased after the low, wind directions were used to classify the event type (follow arrow from Temperature Gradient to Wind Direction, Fig. 11). If the temperature decreased, the storm was classified as a cold front. Often, these cold fronts were associated with a secondary system and this could allow multiple low pressure systems during the same wave event. If so, a further test was carried out to classify the associated front following the same procedure, typically showing up as a warm front or a low-pressure system.

In general, cold fronts were the easiest to identify because they significantly alter the local meteorological conditions. They were defined in the first round of the classification scheme as a low in pressure and followed by a drop in temperature, and in the second round of the classification scheme as a change in wind direction from north/northeastward to south/southwestward. No occurrences of a cold front defined in the first round were reclassified in the second round using the wind data.

While low-pressure systems can have a large pressure change associated with them, there are cases where the storm center moves offshore from the recording station and no front passes over the area and the change in pressure recorded may be minimal. On the other hand low-pressure system storm wind patterns were found to be more consistent than those associated with the other weather systems, and thus more reliably identified. Due to this, low-pressure systems were classified in the second round of the scheme. They are defined as having winds predominantly towards the south, or in the case of a stronger storm passing nearby, a change in wind direction from southward to northward. "Backdoor" low-pressure systems those moving over land from west to east, may be missed by this classification scheme as the change in wind direction will be converse.

Warm fronts often preceded or closely followed a cold front, or were associated with low-pressure systems, which caused them to be the most difficult to classify. Events with wind patterns that did not adhere to the conditions for cold fronts or low-pressure systems were classified as warm fronts.

3.4.5. *Classification scheme accuracy*

The classification scheme was used to analyze data from buoy 41004 for each year during the period 1994–2006. For the years 2001–2006, manual changes were made for storms that appeared to be identified incorrectly. Suspect storms were compared with Unisys and NOAA composite surface weather maps before being manually corrected. Daily weather maps were not consistently available for the years 1994–2000, so no manual corrections were made in that period. To further assess the accuracy of the classification scheme, the classifications for each low-pressure event at buoy 41004 during the years 2003 and 2004 were closely evaluated in comparison with composite surface maps from Unisys and NOAA. Discrepancies were manually changed. On average there were approximately 10% of the storms associated with low-pressure systems that needed to be changed. For the low-pressure type storm systems, the National Climatic Data Center (NCDC) records of storms impacting the Carolinas from 1994 to 2006 (http://www4.ncdc.noaa.gov/cgi-win/wwcgi.dll?wwevent~storms) were compared with the classifications for these years. Except for a few "backdoor" storms, all the storms recorded by the NCDC were correctly identified by the classification scheme.

4. Discussion

The total number of storms and type of event (cold front, warm front, or low-pressure) from 1994 to 2006 are shown in Table 2. Yearly statistics indicate generally low inter-annual variability. On average, there were 100 storms per year, including 40 cold fronts, 33 warm fronts, and 26 low-pressure systems. Only a few systems were undefined. This produces a "storm" on average every 3 days, and this frequency of occurrence can be seen in Fig. 12A based on the wave height (red line). Percentages for each type of front were calculated as the total number of hours

Table 2
Storm analysis using NDBC buoy 41004 with NARR data filling the gaps. Number, total, and percent of each type of storm type is presented from 1994–2006, as well as averages over years without WW3 data (1994–2000), with WW3 data (2001–2006), and for all years (1994–2006). *=no WW3 data available for these years, run without manual corrections due to inconsistent availability of daily weather maps prior to 2001.

Year	Cold	Warm	Low-pressure	Undefined	# storms	% cold	% warm	% Low-pressure
1994**	34	41	26	0	101	34	43	23
1995**	43	23	33	0	99	42	26	32
1996**	39	35	17	0	91	39	41	20
1997**	52	27	22	0	101	51	26	22
1998**	42	31	27	0	100	43	29	28
1999**	38	28	27	0	93	40	32	28
2000**	44	33	28	0	105	40	32	28
2001	42	27	28	0	97	42	31	27
2002	37	38	31	0	106	32	39	29
2003	45	35	24	0	104	38	37	24
2004	38	36	23	1	98	39	36	25
2005	39	29	19	1	88	43	30	26
2006	39	35	28	0	102	42	31	26
1994–2000 avg.	42	31	26	0	99	41	33	26
1994–2006 avg.	41	32	26	0	99	40	33	26
2001–2006 avg.	40	33	26	0	99	39	34	26

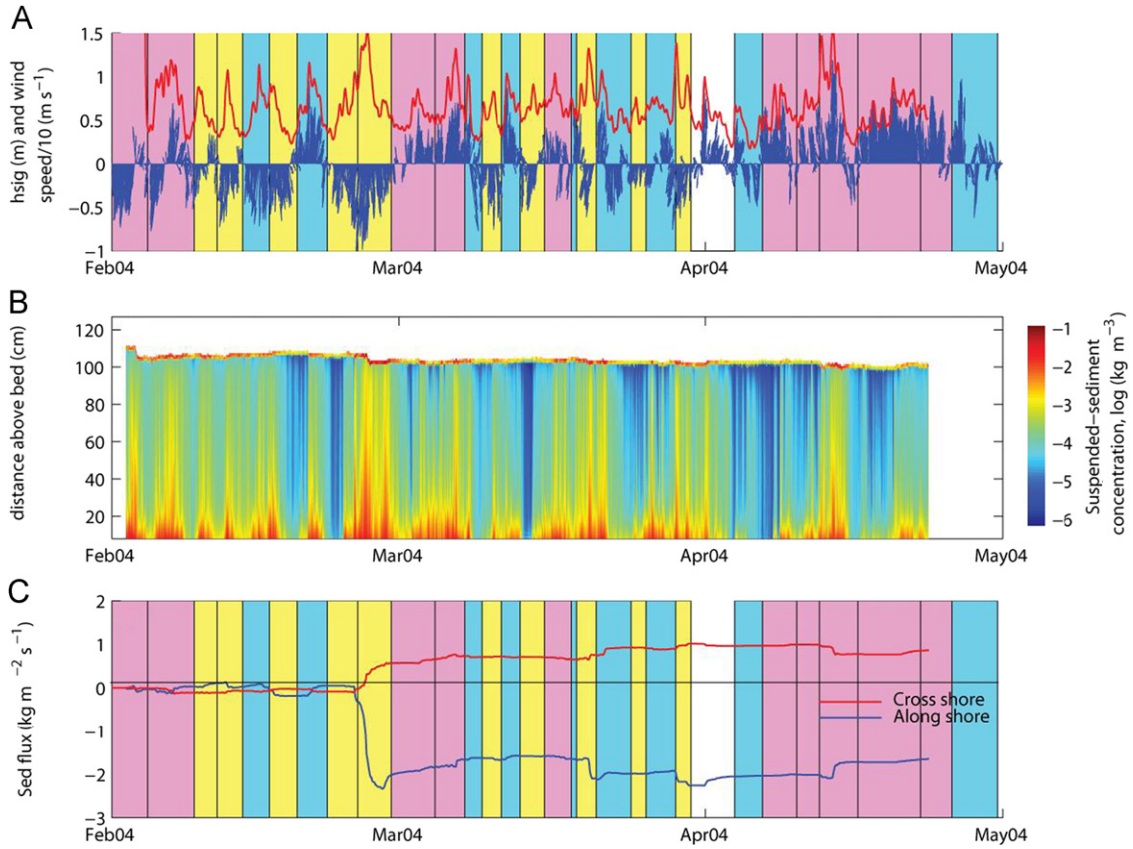

Fig. 12. Deployment period storm analysis. (A) significant wave height (red line) and wind speed and direction (arrows). Shading represents storm type (blue=cold front, red=warm front, yellow= low-pressure). (B) Vertical profiles of suspended-sediment concentration. (C) Cumulative along-shore and cross-shore sediment flux. (For interpretation of the references to color in this figure legend, the reader is referred to the web version of this article.)

defined as each type of storm divided by the total number of hours for which data was collected during the year. Because each year had on average about 100 storms, this equates to approximately the same percentages of storm occurrence (40%, 33%, and 26%, for cold, warm, and low-pressure systems, respectively). During the deployment period, there were 9 cold fronts, 10 warm fronts, and 10 low-pressure systems (Fig. 12A), representing on an average about 33% of the time for each type of system. The results correlate well with the longer term averages (10 years), except for the slightly higher percentage of low-pressure systems. The record shows that February was marked with more cold front and low-pressure type events and as the season progressed more warm fronts occurred in April into May. The impact of the storm types on net sediment flux is computed as the depth-average near-bottom concentration from the ABS's (Fig. 12B) multiplied by the near-bed velocity from the ADV's. The cumulative sediment flux (Fig. 12C) is divided into alongshore and cross shore directions. The alongshore component is driven primarily to the south–west during the low-pressure systems, with a component to the north–east during the cold and warm fronts.

The magnitude of cumulative sediment flux change from the low-pressure systems is typically greater than the cold or warm fronts because the transport during these events is unidirectional. During the deployment period, the majority of the transport occurred during one of these strong low-pressure type systems at the end of February. During cold and warm events, the sediment fluxes oscillate so the net transport will be reduced compared to the low-pressure systems. For this study period, the net along-shore directed transport was towards the south–west. In the cross-shore direction, the net sediment flux is not as strong but tends to show an onshore-directed component. These observational measurements of suspended sediment are inherently difficult to measure due to uncertainties in grain size, spatial variability of sediment characteristics, and errors in measurements. The accuracy of the instruments are listed in Table 1. Additionally the methods used here are focused on suspended load, and may not take into account the bed load transport. However, the responses of the storm as observed with the sonar imagery identify similar trends as those computed from the suspended-sediment fluxes.

Qualitative assessments of sediment transport directions on the inner-continental shelf of Long Bay were inferred from modern sediment distribution, bedform morphology, and sediment textural variations (Baldwin et al., 2006; Denny et al., 2005; Denny et al., in press). Although, observations made from high-resolution seafloor mapping data likely apply to longer temporal scales than observed in this paper, their assessment supports the main conclusion of the observational study; that medium- to fine-grained, sandy sediments are generally transported along-shore to the south–west, leaving behind coarser grained sand as a winnowed lag deposit.

5. Conclusions

Long Bay is a sediment-starved embayment along the US East Coast in South Carolina where rates and pathways of sediment transport are important to coastal communities as a fundamental component of the coastal sediment budget for use in beach nourishment projects, seafloor habitat, and commercial and recreational marine navigation.

Sediment dynamics in the Long Bay region are strongly influenced by local storms, which produce the wind and wave forcings needed to suspend and transport sediment. The three predominant types of storms that affect the region include cold fronts, warm fronts, and low-pressure systems. The type of front/storm and duration of the event determine the direction and magnitude of net sediment flux.

During the passage of cold fronts, winds shift from northeastward to southwestward. Wave height, wave period, and bottom orbital velocities are strongest on the leading edge of the storm because the winds have a longer fetch. Sediments in suspension are driven northeastward. During the passage of warm fronts, winds shift from southwestward to northeastward. Wave height, wave period, and bottom orbital velocities tend to be stronger after the passage of the front than before the front. Sediments in suspension are driven northeastward. During the passage of low-pressure systems, winds shift from southwestward to southeastward. Wave height, wave period, and bottom orbital velocities increase with southwestward winds. After the wind shifts to southeastward, wave height and bottom orbital velocities begin to decrease. Sediment is in suspension for the duration of the storm, and driven southwestward by strong southwestward currents.

Both warm fronts and cold fronts provide a mechanism by which sediments are transported northeastward. This transport is the summation of alternating flows which leads to a lower net movement of sediment. However, powerful low-pressure systems will transport sediments southwestward in a constant uni-directional pattern. During this study period, the net sediment flux was towards the south–west in the alongshore direction and onshore in the cross shore direction.

The magnitude and frequency with which warm fronts, cold fronts, and low-pressure systems pass through Long Bay are of great significance to the development of regional sediment budgets, and understanding of these processes will lead to more successful management of sediment and coastal resources. Connections between inner-continental shelf processes and nearshore processes are still uncertain and require further investigation.

Acknowledgments

A collaborative effort with the US Geological Survey, the University of South Carolina, and Georgia Institute of Technology Savannah conducted three cruises aboard the R/V Dan Moore, owned and operated by Cape Fear Community College, to deploy and recover individual instruments on 26 moorings to obtain this data set. This research was funded by the South Carolina Coastal Erosion Project (http://pubs.usgs.gov/fs/2005/3041/), a cooperative study supported by the US Geological Survey and the South Carolina Sea Grant Consortium (Sea Grant Project no: R/CP-11).

References

Atkinson, L.P., Menzel, D.W., 1985. Introduction: oceanography of the southeast United States continental shelf. In: Atkinson, L.P., Menzel, D.W., Bush, K.A. (Eds.), Oceanography of the Southeast U S Continental Shelf. Coastal and Estuarine Science 2, 1–9. AGU.

Atkinson, L.P., Lee, T.N., Blanton, J.O., Chandler, W.S., 1983. Climatology of southeastern United States continental shelf waters. Journal of Geophysical Research 88 (C8), 4705–4718.

Austin, J.A., Lentz, S.J., 1999. The relationship between synoptic weather systems and meteorological forcing on the North Carolina inner shelf. Journal of Geophysical Research 104 (C8), 18159–18185.

Baldwin, W.E., Morton, R.A., Denny, J.F., Dadisman, S.V., Schwab, W.C., Gayes, P.T., Driscoll, N.W., 2004. Maps Showing the Stratigraphic Framework of South Carolina's Long Bay from Little River to Winyah Bay. US Geological Survey Open-File Report 2004-1013, p. 28.

Baldwin, W.E., Morton, R.A., Putney, T.R., Harris, M.S., Driscoll, N.W., Denny, J.F., Schwab, W.C., 2006. Migration of the Pee Dee River system inferred from ancestral paleochannels underlying the South Carolina Grand Strand and Long Bay inner shelf. Geological Society of America Bulletin 118, 533–549.

Barnhardt, W., Denny, J., Baldwin, W., Schwab, W., Morton, R., Gayes, P., Driscoll, N., 2007. Geologic framework of the Long Bay inner shelf: implications for coastal evolution in South Carolina. In: Proceedings of the Coastal Sediments 2007, New Orleans, vol. 3, pp. 2151–2163.

Blanton, J.O., 1981. Ocean currents along a nearshore frontal zone on the continental shelf of the southeastern United States. Journal of Physical Oceanography 11, 1627–1637.

Blanton, J.O., Atkinson, L.P., 1983. Transport and fate of river discharge on the continental shelf off the southeastern United States. Journal of Geophysical Research 88, 4730–4738.

Denny, J.F., Baldwin, W.E., Schwab, W.C., Gayes, P.T., Morton, R.A., Driscoll, N.W., 2005. Morphology and Textures of Modern Sediments on the Inner Shelf of South Carolina's Long Bay from Little River Inlet to Winyah Bay. US Geological Survey Open-File Report 2005-1345, p. 56.

Denny, J.F., Schwab, W.C., Baldwin, W.E., Barnhardt, W.A., Gayes, P.T., Morton, R.A., Warner, J.C., Driscoll, N.W., Harris, M.S., Wright, E.E., Volgaris, G., Katuna, M.P., Putney, T.R. Distribution of modern sediment deposits on the inner continental shelf of Long Bay, South Carolina, Little River Inlet to Winyah Bay. Implications for coastal evolution, in press.

Gutierrez, B.T., Voulgaris, G., Work, P.A., 2006. Cross-shore variation of wind-driven flows on the inner shelf in Long Bay, South Carolina, USA. Journal of Geophysical Research Oceans 111, C03015, http://dx.doi.org/10.1029/2005JC003121.

Lee, T.N., Kourafalou, V., Wang, J.D., Ho, W.J., Blanton, J.O., Atkinson, L.P., Pietrafesa, L.J., 1985. Shelf circulation from Cape Canaveral to Cape Fear during winter. In: Atkinson, L.P., Menzel, D.W., Bush, K.A. (Eds.), Oceanography of the Southeastern US Continental Shelf: Coastal and Estuarine Sciences, 2. American Geophysical and Geophysics Union, Washington DC, pp. 33–62.

Lee, T.N., Brooks, D.A., 1979. Initial observations of current, temperature, and coastal sea level pressure to atmospheric and Gulf Stream forcing on the Georgia shelf. Geophysical Research Letters 6, 321–324.

Madsen, O.S., 1994. Spectral wave-current bottom boundary layer flows. Coastal engineering 1994. In: Proceedings of the 24th International Conference, Coastal Engineering Research Council, ASCE, pp. 384–398.

Pietrafesa, L.J., Janowitz, G.S., Wittman, P.A., 1985. Physical oceanographic processes in the Carolina Capes. In: Atkinson, L.P., Menzel, D.W., Bush, K.A. (Eds.), Oceanography of the Southeastern US Continental Shelf, Coastal and Estuarine Sciences, 2. American Geophysical Union, Washington DC, pp. 23–32.

Poppe, L.J., Eliason, A.H., Fredricks, J.J., 1985. APASA-An automated particle size analysis system. US Geological Survey Circular 963, 7.

Schwing, F.B., Kjerfve, B., Sneed, J.E., 1983. Nearshore coastal currents on the South Carolina continental shelf. Journal of Geophysical Research 88, 4719–4729.

Schwab, W.C., Gayes, P.T., Morton, R.A., Driscoll, N.W., Baldwin, W.E., Barnhardt, W.A., Denny, J.F., Harris, M.S., Katuna, M.P., Putney, T.R., Voulgaris, G., Warner, J.C., E.E., Wright, 2008. Barnhardt, W. (Ed.), Coastal Change Along the Shore of Northeastern South Carolina: The South Carolina Coastal Erosion Study. US Geological Survey Open-File Report 2008-1206.

Sullivan, C.M., Warner, J.C., Martini, M.A., Voulgaris, G., Work, P.A., Haas, K.A., Hanes, D.H., 2006. South Carolina Coastal Erosion Study Data Report for Observations October 2003–April 2004. US Geological Survey Open-File Report 2005-1429 DVD-ROM, 〈http://pubs.usgs.gov/of/2005/1429/〉.

Soulsby, R.L., Whitehouse, R.J.S., 1997. Threshold of sediment motion in Coastal Environments. In: Proceedings of Combined Australasian Coastal Engineering and Ports Conference, Christchurch, 1997.

Tebeau, P., T.N., Lee, 1979. Wind-induced circulation on the Georgia shelf (December 1976–November 1977). University of Miami Tech. Rep. UM RSMAS 79003, 87.

Thorne, P.D., Hanes, D.M., 2002. A review of acoustic measurement of small-scale sediment processes. Continental Shelf Research 22, 603–632.

Thorne, P.D., Campbell, S.C., 1992. Backscattering by a suspension of spheres. Journal of the Acoustical Society of America 92, 978–986.

Voulgaris, G., Morin, J., 2008. A long-term real Time sea bed morphology evolution system in the South Atlantic Bight. In: Proceedings of the IEEE/OES CMTC Ninth Working Conference on Current Measurement Technology, pp. 71–79.

Werner, F.E., Blanton, J.O., Lynch, D.R., Savidge, D.K., 1993. A numerical study of the continental shelf circulation of the US South Atlantic Bight during the autumn of 1987. Continental Shelf Research 13, 871–997.